



# Soluble TREM2 in CSF and its association with other biomarkers and cognition in autosomal-dominant Alzheimer's disease: a longitudinal observational study

Estrella Morenas-Rodríguez, Yan Li, Brigitte Nuscher, Nicolai Franzmeier, Chengjie Xiong, Marc Suárez-Calvet, Anne M Fagan, Stephanie Schultz, Brian A Gordon, Tammie L S Benzinger, Jason Hassenstab, Eric McDade, Regina Feederle, Celeste M Karch, Kai Schlepckow, John C Morris, Gernot Kleinberger, Bengt Nellgard, Jonathan Vöglein, Kaj Blennow, Henrik Zetterberg, Michael Ewers, Mathias Jucker, Johannes Levin, Randall J Bateman, Christian Haass, on behalf of the Dominantly Inherited Alzheimer Network

## Summary

**Background** Therapeutic modulation of TREM2-dependent microglial function might provide an additional strategy to slow the progression of Alzheimer's disease. Although studies in animal models suggest that TREM2 is protective against Alzheimer's pathology, its effect on tau pathology and its potential beneficial role in people with Alzheimer's disease is still unclear. Our aim was to study associations between the dynamics of soluble TREM2, as a biomarker of TREM2 signalling, and amyloid  $\beta$  ( $A\beta$ ) deposition, tau-related pathology, neuroimaging markers, and cognitive decline, during the progression of autosomal dominant Alzheimer's disease.

**Methods** We did a longitudinal analysis of data from the Dominantly Inherited Alzheimer Network (DIAN) observational study, which includes families with a history of autosomal dominant Alzheimer's disease. Participants aged over 18 years who were enrolled in DIAN between Jan 1, 2009, and July 31, 2019, were categorised as either carriers of pathogenic variants in *PSEN1*, *PSEN2*, and *APP* genes (n=155) or non-carriers (n=93). We measured amounts of cleaved soluble TREM2 using a novel immunoassay in CSF samples obtained every 2 years from participants who were asymptomatic (Clinical Dementia Rating [CDR]=0) and annually for those who were symptomatic (CDR>0). CSF concentrations of  $A\beta_{40}$ ,  $A\beta_{42}$ , total tau (t-tau), and tau phosphorylated on threonine 181 (p-tau) were measured by validated immunoassays. Predefined neuroimaging measurements were total cortical uptake of Pittsburgh compound B PET (PiB-PET), cortical thickness in the precuneus ascertained by MRI, and hippocampal volume determined by MRI. Cognition was measured using a validated cognitive composite (including DIAN word list test, logical memory delayed recall, digit symbol coding test [total score], and minimal status examination). We based our statistical analysis on univariate and bivariate linear mixed effects models.

**Findings** In carriers of pathogenic variants, a high amyloid burden at baseline, represented by low CSF  $A\beta_{42}$  ( $\beta=-4.28 \times 10^{-2}$  [SE 0.013],  $p=0.0012$ ), but not high cortical uptake in PiB-PET ( $\beta=-5.51 \times 10^{-3}$  [0.011],  $p=0.63$ ), was the only predictor of an augmented annual rate of subsequent increase in soluble TREM2. Augmented annual rates of increase in soluble TREM2 were associated with a diminished rate of decrease in amyloid deposition, as measured by  $A\beta_{42}$  in CSF ( $r=0.56$  [0.22],  $p=0.011$ ), in presymptomatic carriers of pathogenic variants, and with diminished annual rate of increase in PiB-PET ( $r=-0.67$  [0.25],  $p=0.0060$ ) in symptomatic carriers of pathogenic variants. Presymptomatic carriers of pathogenic variants with annual rates of increase in soluble TREM2 lower than the median showed a correlation between enhanced annual rates of increase in p-tau in CSF and augmented annual rates of increase in PiB-PET signal ( $r=0.45$  [0.21],  $p=0.035$ ), that was not observed in those with rates of increase in soluble TREM2 higher than the median. Furthermore, presymptomatic carriers of pathogenic variants with rates of increase in soluble TREM2 above or below the median had opposite associations between  $A\beta_{42}$  in CSF and PiB-PET uptake when assessed longitudinally. Augmented annual rates of increase in soluble TREM2 in presymptomatic carriers of pathogenic variants correlated with decreased cortical shrinkage in the precuneus ( $r=0.46$  [0.22]),  $p=0.040$ ) and diminished cognitive decline ( $r=0.67$  [0.22],  $p=0.0020$ ).

**Interpretation** Our findings in autosomal dominant Alzheimer's disease position the TREM2 response within the amyloid cascade immediately after the first pathological changes in  $A\beta$  aggregation and further support the role of TREM2 on  $A\beta$  plaque deposition and compaction. Furthermore, these findings underpin a beneficial effect of TREM2 on  $A\beta$  deposition,  $A\beta$ -dependent tau pathology, cortical shrinkage, and cognitive decline. Soluble TREM2 could, therefore, be a key marker for clinical trial design and interpretation. Efforts to develop TREM2-boosting therapies are ongoing.

**Funding** German Research Foundation, US National Institutes of Health.

**Copyright** © 2022 The Author(s). Published by Elsevier Ltd. This is an Open Access article under the CC BY-NC-ND 4.0 license.

*Lancet Neurol* 2022; 21: 329–41  
See [Comment](#) page 297

This online publication has been corrected. The corrected version first appeared at [thelancet.com/neurology](http://thelancet.com/neurology) on April 13, 2022

German Center for Neurodegenerative Diseases, Munich, Germany (E Morenas-Rodríguez MD, B Nuscher BSc, R Feederle PhD, K Schlepckow PhD, G Kleinberger PhD, J Vöglein MD, Prof M Ewers PhD, Prof J Levin MD, Prof C Haass PhD); Metabolic Biochemistry, Biomedical Center, Faculty of Medicine (E Morenas-Rodríguez, B Nuscher, K Schlepckow, G Kleinberger, Prof C Haass), Institute for Stroke and Dementia Research, Klinikum der Universität München (N Franzmeier PhD, Prof M Ewers), Department of Neurology, University Hospital of Munich (J Vöglein, Prof J Levin), Ludwig-Maximilians University, Munich, Germany; Division of Biostatistics (Yan Li PhD, Prof C Xiong PhD), Department of Neurology (Prof A M Fagan PhD, Prof J Hassenstab PhD, Prof E McDade DO, Prof J C Morris MD, Prof R J Bateman MD), Mallinckrodt Institute of Radiology (S Schultz PhD, B A Gordon PhD, Prof T L S Benzinger MD), Department of Psychiatry (Prof C M Karch PhD), Washington University School of Medicine, St Louis, MO, USA; BarcelonaBeta Brain Research Center, Pasqual Maragall Foundation, Barcelona, Spain (M Suárez-Calvet PhD); Servei de Neurologia, Hospital del Mar Medical Research Institute, Barcelona, Spain (M Suárez-Calvet); Centro de

Investigación Biomédica en Red de Fragilidad y Envejecimiento Saludable, Madrid, Spain (M Suárez-Calvet); Munich Cluster for Systems Neurology (SyNergy), Munich, Germany (R Feederle, Prof J Levin, Prof C Haass); Institute for Diabetes and Obesity, Monoclonal Antibody Core Facility, Helmholtz Center, Munich, Germany (R Feederle); German Research Center for Environmental Health, Neuherberg, Germany (R Feederle); Department of Anesthesiology and Intensive Care, Sahlgrenska University Hospital, Mölndal, Sweden (B Nellgard MD); Institute of Clinical Sciences (B Nellgard) and Department of Psychiatry and Neurochemistry (K Blennow MD, H Zetterberg MD), Sahlgrenska Academy, University of Gothenburg, Gothenburg, Sweden; Clinical Neurochemistry Laboratory, Sahlgrenska University Hospital, Mölndal, Sweden (K Blennow, H Zetterberg); Department of Neurodegenerative Disease, UCL Queen's Square Institute of Neurology (H Zetterberg) and UK Dementia Research Institute (H Zetterberg), University College London, London, UK; Hong Kong Center for Neurodegenerative Diseases, Hong Kong Special Administrative Region, China (H Zetterberg); German Center for Neurodegenerative Diseases, Tübingen, Germany (M Jucker PhD); Department of Cellular Neurology, Hertie Institute for Clinical Brain Research, Tübingen, Germany (M Jucker)

Correspondence to: Dr Estrella Morenas-Rodríguez, Memory Unit, Department of Neurology, Hospital Universitario 12 de Octubre, Madrid 28041, Spain  
estrella.morenas.rodriguez@gmail.com

## Research in context

### Evidence before this study

We searched PubMed from database inception to October, 2021, with the terms “sTREM2”, “soluble TREM2” AND “Alzheimer’s Disease” OR “Alzheimer” OR “Alzheimer’s”, with no language restrictions. Studies that focused on animal models or non-Alzheimer’s disease neurodegenerative diseases were excluded. Previous cross-sectional studies have consistently shown an elevation of soluble TREM2 in CSF in late presymptomatic and early symptomatic phases of Alzheimer’s disease, both in sporadic and autosomal dominant cases. Based on these cross-sectional findings, a temporal change in soluble TREM2 over the development of Alzheimer’s disease was inferred, with a peak around symptom onset. These studies also found a high correlation between tau-related markers in CSF (total tau [t-tau] and phosphorylated tau on threonine 181 [p-tau]) and soluble TREM2 in CSF. Some early studies, focusing on the symptomatic phase of sporadic Alzheimer’s disease, suggested that higher baseline soluble TREM2 levels in CSF were associated with a more benign disease progression concerning hippocampal shrinkage and memory functions, whereas other studies found a correlation with worsening of cognitive and functional scores. Nevertheless, in sporadic Alzheimer’s disease, higher baseline levels of soluble TREM2 were associated with slower amyloid- $\beta$  peptide (A $\beta$ ) deposition, as measured by amyloid-PET imaging. All current studies have assessed soluble TREM2 levels in CSF in a cross-sectional manner and, therefore, have not captured the dynamics of the TREM2 response within Alzheimer’s disease from the very early presymptomatic phase. Thus, the triggers and effects related to the longitudinal increase in soluble TREM2 levels in CSF in people with Alzheimer’s disease remain elusive.

### Added value of this study

The longitudinal analysis of autosomal dominant Alzheimer’s disease incorporated into the design of this study gave us the unique opportunity to investigate the dynamics of soluble TREM2 in CSF and its effects on Alzheimer’s disease progression in a well characterised cohort from the presymptomatic phase of the disease. To the best of our knowledge, this is the first study not only to assess the dynamics of soluble TREM2 longitudinally in Alzheimer’s disease, and its association with amyloid and tau markers, neuroimaging features, and cognition, but also to investigate the effects of increased TREM2 activation during the presymptomatic phase of Alzheimer’s disease. We used a

novel immunoassay that could selectively detect soluble TREM2 generated from the signalling competent full-length cell surface protein by cleavage with ADAM10 and ADAM17. Other soluble TREM2 isoforms generated by alternative splicing were not detected by our novel immunoassay. Therefore, it provides a more accurate measurement of TREM2-dependent microglial activation.

### Implications of all the available evidence

The longitudinal increase in soluble TREM2 levels in carriers of pathogenic variants is related to diminished baseline amounts in CSF of A $\beta$ 42 and the ratio of A $\beta$ 42 to A $\beta$ 40, but not to augmented cortical uptake of the amyloid-PET tracer nor to other markers of tau-related pathology or neuronal death. Consistent with data from animal models, therefore, very early A $\beta$  deposition might be the main trigger of soluble TREM2 elevation. The noted amyloid-dependent protective effect of TREM2 on tau pathology in people with autosomal dominant Alzheimer’s disease accords with novel findings in mouse models. The rate of increase in soluble TREM2 significantly modified the association between longitudinal changes in A $\beta$ 42 in CSF and longitudinal changes in PiB-PET uptake, supporting a function of TREM2 on amyloid clearance and A $\beta$  plaque compaction, as also suggested by animal models. This finding highlights the potential clinical use of soluble TREM2 for the interpretation of both these amyloid markers. Importantly, we found that an augmented longitudinal rate of increase in soluble TREM2 during the presymptomatic phase of autosomal dominant Alzheimer’s disease correlated with slower cortical shrinkage in the precuneus and slower cognitive decline. Therefore, our findings clarify previous contradictory cross-sectional results regarding the effects of TREM2 on neurodegeneration and cognition, and indicate a protective function of TREM2, particularly in the presymptomatic phase of Alzheimer’s disease. These findings support ongoing efforts to develop TREM2-boosting therapies as disease-modifying treatments for Alzheimer’s disease and suggest an early window for therapeutic intervention. Moreover, these results highlight the relevance of soluble TREM2 in CSF as a key marker in the design and interpretation of anti-amyloid clinical trials, due to its tight association with amyloid-related pathological processes and cognition. Finally, the available knowledge on TREM2 function allows for the integration of protective microglial activities into the amyloid cascade by placing them right after initial A $\beta$  deposition.

## Introduction

Microglia were at one time believed to primarily contribute to Alzheimer’s disease progression.<sup>1</sup> However, single-cell sequencing technologies have identified dynamic microglial populations that sense their environment and trigger defensive responses to Alzheimer’s disease

pathology.<sup>2</sup> Moreover, large genome-wide association studies have identified loss-of-function variants in the protein TREM2, which are associated with an increased risk for late onset Alzheimer’s disease.<sup>3,4</sup> Loss of TREM2 function locks microglia in a homeostatic state and prevents their switch to disease-associated microglia.<sup>2,5</sup>

Because disease-associated microglia facilitate lipid metabolism, efficiently remove amyloid  $\beta$  ( $A\beta$ ) seeds, and form a barrier around  $A\beta$  plaques, their protective activities are now being investigated in the development of disease-modifying therapeutic strategies.<sup>6</sup> It is, therefore, important to translate our knowledge on protective TREM2 functions from animal models to patients with Alzheimer's disease. Quantitative analysis of soluble TREM2 in CSF allows such translational efforts. We have previously shown that cell-surface full-length TREM2 is shed by proteases of the ADAM family, releasing soluble TREM2 into biological fluids, including CSF, of patients with Alzheimer's disease.<sup>4,7</sup> Because only cell-surface full-length TREM2 is capable of efficiently initiating downstream signalling, and ADAM proteases cleave TREM2 preferentially on the plasma membrane,<sup>4,7</sup> soluble TREM2 in CSF can be considered as a biomarker for TREM2 expression and signalling.

Cross-sectional studies have shown that soluble TREM2 levels in CSF are increased in late presymptomatic and early symptomatic stages of Alzheimer's disease, both in sporadic and in autosomal dominant cases.<sup>8–10</sup> However, it remains unclear whether augmented baseline soluble TREM2 levels are associated with less neurodegeneration compared with lower baseline concentrations, as measured by neuroimaging, and less cognitive decline in symptomatic phases of sporadic late onset Alzheimer's disease.<sup>11–17</sup> Furthermore, cross-sectional analysis of soluble TREM2 levels is affected by high interindividual variability and only estimates the microglial activation state at a single timepoint—it does not represent the dynamic TREM2-dependent microglial response during Alzheimer's disease progression. Longitudinal studies are better able to accurately investigate the pathological processes occurring in Alzheimer's disease, because this study design can enable discrimination between temporal changes in biomarkers representing these pathological processes and their dynamic associations.<sup>18,19</sup> Only two studies have, thus far, investigated longitudinal changes in soluble TREM2 levels,<sup>20,21</sup> but none of them focused on individuals with an Alzheimer's disease diagnosis or presymptomatic individuals developing Alzheimer's disease.

On the basis of amyloid PET-imaging studies and seeding experiments in mice,<sup>22</sup> beneficial TREM2-dependent microglial functions are expected to be most effective in the earliest stages of  $A\beta$  deposition, which has not yet been studied in people with Alzheimer's disease. Studying this initial stage of disease is possible in individuals with autosomal dominant Alzheimer's disease, because carriers of pathogenic variants have a predictable clinical onset in each family, and penetrance of the involved mutations is mostly complete.<sup>23</sup> This near-complete penetrance means that individuals with autosomal dominant Alzheimer's disease can be staged relative to their expected year of symptom onset, and biomarker dynamics can be studied from the very early presymptomatic phase of disease.

The Dominantly Inherited Alzheimer Network (DIAN) observational study recruits participants from families who have a history of autosomal dominant Alzheimer's disease, many of whom have longitudinal markers of  $A\beta$  deposition, tau-related pathology, neuronal death and dysfunction, and longitudinal cognitive evaluations.<sup>24</sup> Here, using participants in DIAN, we aimed to study longitudinal changes in levels of soluble TREM2 in CSF throughout the course of Alzheimer's disease. We also aimed to explore longitudinally the association between soluble TREM2 in CSF and other biomarkers of Alzheimer's disease, to find the triggers of soluble TREM2, to explore potential protective activities of TREM2 during the presymptomatic phase of Alzheimer's disease, and to identify a window for therapeutic modulation of TREM2 (appendix p 6).

See Online for appendix

## Methods

### Study design and participants

The DIAN observational study was launched in 2008 and is a well described longitudinal and international study at 17 sites in Argentina, Australia, Germany, Spain, the UK, and the USA. Methods for this cohort study have already been described.<sup>24</sup> DIAN recruits families with a history of autosomal dominant Alzheimer's disease. Participants are categorised as either non-carriers or carriers of pathogenic variants in *PSEN1*, *PSEN2*, and *APP* genes. The DIAN study is supervised by the institutional review board at Washington University (St Louis, MO, USA), which provided human studies ethics approval. Participants or their caregivers provided written informed consent in accordance with their local institutional review board.

For our study, all participants with genetic, clinical, CSF, and neuroimaging longitudinal data that passed quality control from the 14th data freeze (2009–19) were included for quantification of soluble TREM2 in CSF. Families carrying the *APP* (E693G; Dutch) mutation were excluded from the statistical analysis ( $n=13$ ), as these mutations often present with predominant cerebral amyloid angiopathy and diffuse  $A\beta$  plaques with little neurofibrillary tangle pathology.<sup>23,25</sup> The estimated years from symptom onset (EYO) were calculated for each visit for both groups (carriers of pathogenic variants and non-carriers) as the participant's current age relative to parental age at first progressive cognitive decline.<sup>24</sup> Further details about the cohort and protocol are provided in the appendix (p 1).

### Procedures

Participants underwent a comprehensive clinical and neuropsychological evaluation.<sup>24</sup> Dementia status was determined by the Clinical Dementia Rating (CDR).<sup>26</sup> Genetic characterisation and *APOE* genotyping was done as previously described.<sup>24</sup> Clinical evaluators were masked to the carrier status of participants.  $A\beta_{42}$ ,  $A\beta_{40}$ , total tau (t-tau), and tau phosphorylated at threonine 181

(p-tau) were measured by immunoassay, using the Lumipulse platform (Fujirebio, Tokyo, Japan). Further details of these procedures are given in the appendix (p 1).

MRI T1-weighted images were acquired for all participants. In our study, we analysed the averaged measurements of the longitudinal rate of change of cortical thickness in the precuneus and hippocampal volume. Amyloid imaging was done using <sup>11</sup>C-Pittsburgh compound B (<sup>11</sup>C-PiB). Further details about imaging protocols are given in the appendix (p 1).

For quantitative determination of soluble TREM2 concentrations in CSF, we developed a novel Meso Scale Discovery-based immunoassay, which was based on a previously described soluble TREM2 immunoassay.<sup>27</sup> However, to avoid detection of soluble TREM2 variants generated by alternative splicing, we used a novel detection antibody (1H3) that was directed against the neo-epitope on the C-terminus of soluble TREM2, derived by ADAM10 and ADAM17 mediated cleavage of the full-length TREM2 protein. Use of 1H3 allowed us to selectively measure soluble TREM2 derived from the signalling competent cell-surface precursor. We measured 682 CSF samples from 261 participants in duplicates, which were distributed randomly across 19 plates and measured within 3 weeks. Full details of the immunoassay and procedures are given in the appendix (pp 2–5).

### Statistical analysis

Full details of statistical methods are presented in the appendix (pp 7–11). Briefly, amounts of biomarkers in CSF were log-transformed to follow a normal distribution. Cross-sectional analyses focused on descriptive characteristics at baseline of the different clinical groups, including demographic variables and biomarker values at baseline, and were done using  $\chi^2$  tests for categorical variables, and ANOVA or ANCOVA for continuous variables. Age and sex were included as covariates in the ANCOVA, which was done to study the differences between biomarkers at baseline across the different groups. We stratified carriers of pathogenic variants into two groups: presymptomatic carriers of pathogenic variants (ie, participants for whom baseline CDR score was equal to 0) and symptomatic carriers of pathogenic variants (ie, participants for whom baseline CDR score were greater than 0). For studying cognition, we used a cognitive composite, which has been described previously,<sup>28</sup> that is especially sensitive for detection of the slightest changes in cognition during the pre-symptomatic Alzheimer's disease phase. The cognition composite comprised the following tests: DIAN word list test, logical memory delayed recall, digit symbol Coding test (total score), and the Mini-Mental State Examination.

Participants with extreme rates of change in soluble TREM2 levels were defined as those with a raw rate of change in soluble TREM2 higher than the mean plus 3SD or lower than the mean minus 3SD (comprising

seven carriers of pathogenic variants and two non-carriers). The participants with extreme rates of change in soluble TREM2 levels are described in the appendix (pp 18–22). We did the entire analysis by both excluding and including participants with extreme rates of change in soluble TREM2 levels, and both sets of results were highly consistent.

We based our longitudinal analysis on linear mixed effects (LME) models. Univariate LME models were used to assess the effect of baseline biomarkers (predictor) on the longitudinal change of the outcome biomarker. Correlations between the annual rate of change of soluble TREM2 and that of other outcomes were evaluated using bivariate LME models.<sup>29,30</sup> The modification effect of the rate of change of soluble TREM2 on the association between the rates of change in markers of amyloid deposition and tau-related pathology were explored using linear or quadratic regressions.

Statistical analyses were done using SAS version 9.4, PROC GLM, and R version 3.6.1 with ggplot2, ggpubr, lme4, psych, and dplyr packages. All p values were based on two-sided tests, and values less than 0.05 were considered statistically significant.

### Role of the funding source

The funders of the study had no role in study design, data collection, data analysis, data interpretation, or writing of the report.

### Results

Baseline characteristics of the participants are summarised in the table. Cross-sectional soluble TREM2 levels started to be significantly higher in carriers of pathogenic variants than in non-carriers 21 years before the expected symptom onset (figure 1A). However, no timepoint was identified at which the rate of increase in soluble TREM2 was significantly different in carriers of pathogenic variants compared with non-carriers. No modifying effect was noted by sex, level of education, age, or EYO at baseline on the subsequent rate of change in soluble TREM2 in carriers of pathogenic variants and non-carriers (appendix p 11). The mutation status (carriers of pathogenic variants vs non-carriers) and the mutant gene involved (*PSEN1*, *PSEN2*, or *APP*) did not significantly affect the rate of increase in soluble TREM2 (appendix p 11, 12).

Next, low levels of A $\beta$ 42 in CSF, and of the ratio of A $\beta$ 42 to A $\beta$ 40 in CSF, at baseline independently predicted a subsequent augmented annual rate of increase in soluble TREM2 in carriers of pathogenic variants, but not in non-carriers (figure 2A; appendix p 13). By contrast, we did not find any association between total cortical uptake in PiB-PET at baseline and the subsequent annual rate of change in soluble TREM2 (figure 2B; appendix p 13). Amounts of p-tau and t-tau in CSF, and structural MRI biomarkers at baseline, also showed no association with the subsequent longitudinal change in

	Non-carriers (n=91)	Presymptomatic carriers of pathogenic variants (n=100)	Symptomatic carriers of pathogenic variants (n=48)	p value
Age, years	36.3 (11.4)	34.15 (9.5)	46.8 (9.7)	<0.0001*
Sex				
Female	54 (59%)	55 (55%)	25 (52%)	0.69
Male	37 (41%)	45 (45%)	23 (48%)	0.69
Ethnicity				
White†	72 (89%)	77 (85%)	33 (79%)	0.53
Latin American	7 (9%)	8 (9%)	6 (14%)	0.53
Asian	..	4 (4%)	2 (5%)	0.53
Other‡	2 (3%)	1 (2%)	1 (3%)	0.53
APOE ε4 carrier	31 (34%)	33 (33%)	17 (35%)	0.96
EYO, years	-10.0 (12.1)	-13.8 (9.8)	1.9 (6.6)	<0.0001§
Mean follow up, years	3.4 (1.8)	3.4 (1.8)	2.7 (1.7)	0.062
Number of visits with soluble TREM2 determination	..	..	..	0.074
2	63	64	23	..
3	17	25	13	..
4-6	11	11	12	..
Mini-mental state examination, score	28.9 (1.37)	29.1 (1.22)	24.4 (4.4)	<0.0001*
Cognitive composite, z-score	-0.1 (0.9)	-0.2 (0.1)	-2.9 (1.7)	<0.0001*
Years of education	15.0 (2.3)	15.0 (2.8)	14 (3.8)	0.11
CSF variables				
Aβ42, pg/mL	749.6 (263.1)	741.1 (417.0)	381.3 (162.5)	<0.0001*
Aβ40, pg/mL	8484.8 (2792.6)	9028.6 (3305.9)	8636.2 (2711.0)	0.56
Ratio of Aβ42 to Aβ40	0.1 (0.01)	0.1 (0.03)	0.04 (0.01)	<0.0001*
t-tau, pg/mL	267.9 (117.2)	406.5 (289.8)	752.3 (373.2)	<0.0001¶
p-tau, pg/mL	29.8 (16.8)	53.02 (49.0)	127.0 (69.6)	<0.0001¶
Soluble TREM2, ng/mL	2.7 (1.2)	3.4 (1.6)	4.1 (1.3)	<0.0001
Total cortical PiB-PET uptake, SURV	1.07 (0.2)	1.6 (0.8)	3.0 (1.1)	<0.0001¶
Precuneus cortical thickness, mm	2.4 (0.1)	2.4 (0.2)	2.1 (2.2)	<0.0001*
Hippocampal volume, mm <sup>3</sup>	8815.9 (631.5)	8871.4 (752.4)	7497.6 (1246.4)	<0.0001*

Data are mean (SD) or n (%). All p values regarding demographics are based on analysis of raw data (ANOVA). All p values regarding cognitive data (ie, Mini-Mental State Examination and cognitive composite) are adjusted for age and education and based on analysis of raw data (ANCOVA). Categorical variables (ie, sex, APOE status, and visits) were analysed by the  $\chi^2$  test. The p values regarding biochemical markers were based on an analysis (ANCOVA) that considered log-transformed variables and, for raw data, the rest of the variables and neuroimaging markers were adjusted by age and sex. Hippocampal volume was corrected per participant by total brain volume. p values with no footnote relate to comparisons with ANOVA or ANCOVA. EYO=estimated years to symptom onset according to parental onset. PiB-PET=Pittsburgh compound B PET. p-tau=phosphorylated tau on threonine 181. SUVR=standardised uptake value ratio. t-tau=total tau. †Symptomatic carriers of pathogenic variants versus non-carriers of pathogenic variants and presymptomatic carriers of pathogenic variants, p<0.0001. ‡Ethnicity data were available for 214 participants. †Australian aboriginal or native Hawaiian. §Symptomatic carriers of pathogenic variants versus non-carriers of pathogenic variants and presymptomatic carriers of pathogenic variants, p<0.0001; presymptomatic carriers of pathogenic variants versus non-carriers of pathogenic variants, p=0.034. ¶Symptomatic carriers of pathogenic variants versus non-carriers of pathogenic variants and presymptomatic carriers of pathogenic variants, p<0.0001; presymptomatic carriers of pathogenic variants versus non-carriers of pathogenic variants, p<0.0001. ||Non-carriers of pathogenic variants versus presymptomatic carriers, p=0.0026; non-carriers of pathogenic variants versus symptomatic carriers of pathogenic variants, p<0.0001; and presymptomatic carriers of pathogenic variants versus symptomatic carriers of pathogenic variants, p=0.0052. One participant was excluded because of incomplete data.

**Table: Demographic data and biomarker levels at baseline for carriers of pathogenic variants and non-carriers**

soluble TREM2 in carriers of pathogenic variants, nor in non-carriers (figure 2C, D; appendix p 13).

An augmented annual rate of increase in soluble TREM2 correlated with a reduced annual rate of decrease in amounts of Aβ42 in CSF in presymptomatic carriers of pathogenic variants ( $r=0.56$  [SE 0.22],  $p=0.011$ ; figure 3A) and associated with a diminished annual rate of increase in total cortical PiB-PET uptake in symptomatic carriers of pathogenic variants ( $r=-0.67$  [0.25];  $p=0.0060$ ; figure 3B). Regarding markers of tau

pathology, no association was found between the annual rate of increase in soluble TREM2 and the annual rate of change in amounts of t-tau or p-tau (figure 3C, D). However, the annual rate of increase in soluble TREM2 significantly modulated the association between longitudinal changes of p-tau in CSF and longitudinal changes of PiB-PET cortical uptake in presymptomatic carriers of pathogenic variants ( $\beta=-0.394$  [SE 0.137],  $p=0.0056$  for the linear interaction of rate of increase in soluble TREM2 higher than the median  $\times$  annual rate

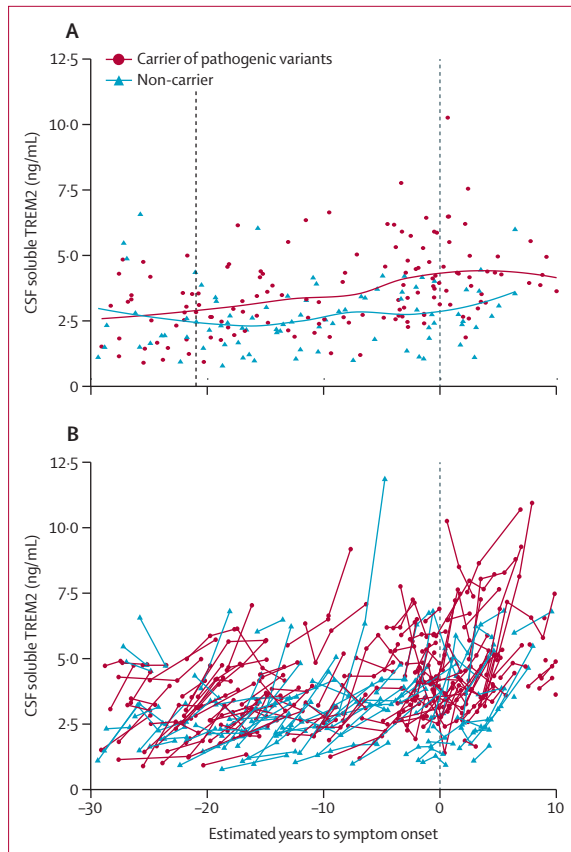


**Figure 1: Cross-sectional and longitudinal soluble TREM2 levels in CSF according to estimated years to symptom onset (EYO) in carriers and non-carriers of pathogenic variants**

(A) Soluble TREM2 baseline levels plotted against EYO at baseline for carriers of pathogenic variants (shown in red,  $n=148$ ) and non-carriers (shown in blue,  $n=91$ ). The dotted line at  $-21$  years indicates the timepoint at which cross-sectional soluble TREM2 levels start to be statistically higher in carriers of pathogenic variants than in non-carriers, according to the method described by McDade and colleagues.<sup>19</sup> The dotted line at 0 years represents the expected point of symptom onset. Lines represent locally weighted scatterplot smoothing (LOESS) best-fitting curves (B) Spaghetti plot showing the longitudinal levels of soluble TREM2 in CSF from carriers of pathogenic variants (depicted by the red line,  $n=148$ ) and non-carriers (depicted by the blue line,  $n=91$ ) as a function of EYO. The dotted line at 0 years represents the expected point of symptom onset. Negative EYO values represent the expected presymptomatic phase. Positive values indicate the expected symptomatic phase of the disease. Because of the low number of participants located at the extremes of the graph, and to maintain their confidentiality, individual participants are not shown in the timeframe before  $-30$  years and after 10 years.

rate of increase in PiB-PET; figures 4A, B; appendix p 14). Presymptomatic carriers of pathogenic variants with annual rates of increase in soluble TREM2 lower than the median showed a correlation between augmented annual rates of increase in p-tau and PiB-PET uptake ( $r=0.45$  [SE 0.21],  $p=0.035$ ; appendix p 15). Conversely, in presymptomatic carriers of pathogenic variants with annual rates of increase in soluble TREM2 higher than the median, no such correlation was seen with higher p-tau increase rate and higher PiB-PET uptake increase rate.

Considering the differential associations between annual rates of increase in soluble TREM2 and amyloid markers ( $A\beta_{42}$  in CSF and PiB-PET uptake), the influence of the annual rate of increase in soluble TREM2 on the association between both these markers was investigated. Presymptomatic carriers of pathogenic variants with an annual rate of increase in soluble TREM2 above the median had opposite associations between annual rates of change in  $A\beta_{42}$  in CSF and in PiB-PET cortical uptake, compared with those with an annual rate of increase in soluble TREM2 lower than the median ( $\beta=0.974$  [SE 0.318],  $p=0.0033$ , for the linear interaction of annual rate of increase in soluble TREM2 higher than the median  $\times$  annual rate of increase in PiB-PET;  $\beta=-6.24$  (1.135),  $p<0.0001$ , for the quadratic interaction; figures 4C, D; appendix p 14). Moreover, the longitudinal change in amount of  $A\beta_{42}$  in CSF was accurately predicted by longitudinal PiB-PET change, when accounting for its interaction with an annual rate of increase in soluble TREM2 above or below the median (adjusted  $r^2=0.45$  vs adjusted  $r^2=0.09$ , without including the interaction; appendix p 15).

Regarding neuroimaging and cognitive outcomes, an augmented annual rate of increase in soluble TREM2 correlated with a reduced annual rate of cortical shrinkage in the precuneus of presymptomatic carriers of pathogenic variants ( $r=0.46$  [SE 0.22],  $p=0.040$ ; figures 5A, B). No association was found between the annual rate of increase in soluble TREM2 and the annual rate of hippocampal shrinkage, in neither presymptomatic carriers of pathogenic variants nor symptomatic carriers of pathogenic variants (figures 5C, D). However, high soluble TREM2 levels at baseline were associated with a decreased annual rate of hippocampal shrinkage (appendix p 16).

A strong correlation was noted between an augmented annual rate of increase in soluble TREM2 and a reduced annual rate of cognitive decline, as measured by a cognitive composite, in presymptomatic carriers of pathogenic variants ( $r=0.67$  [0.22],  $p=0.0020$ ; figures 5E, F).

## Discussion

The DIAN cohort—comprising families affected by autosomal dominant Alzheimer's disease—is ideal for studying changes in Alzheimer's pathology, neuroimaging markers, and cognition over time because of the predictable nature of this form of the disease. We did a longitudinal analysis of data obtained from participants in DIAN, looking at associations between the dynamics of soluble TREM2 and other biomarkers that are known to be associated with progression of Alzheimer's disease. We also assessed cognitive development from very early presymptomatic phases to the late phase with fully developed Alzheimer's disease. The study design of DIAN, with data collected longitudinally, enabled us to make several fundamental

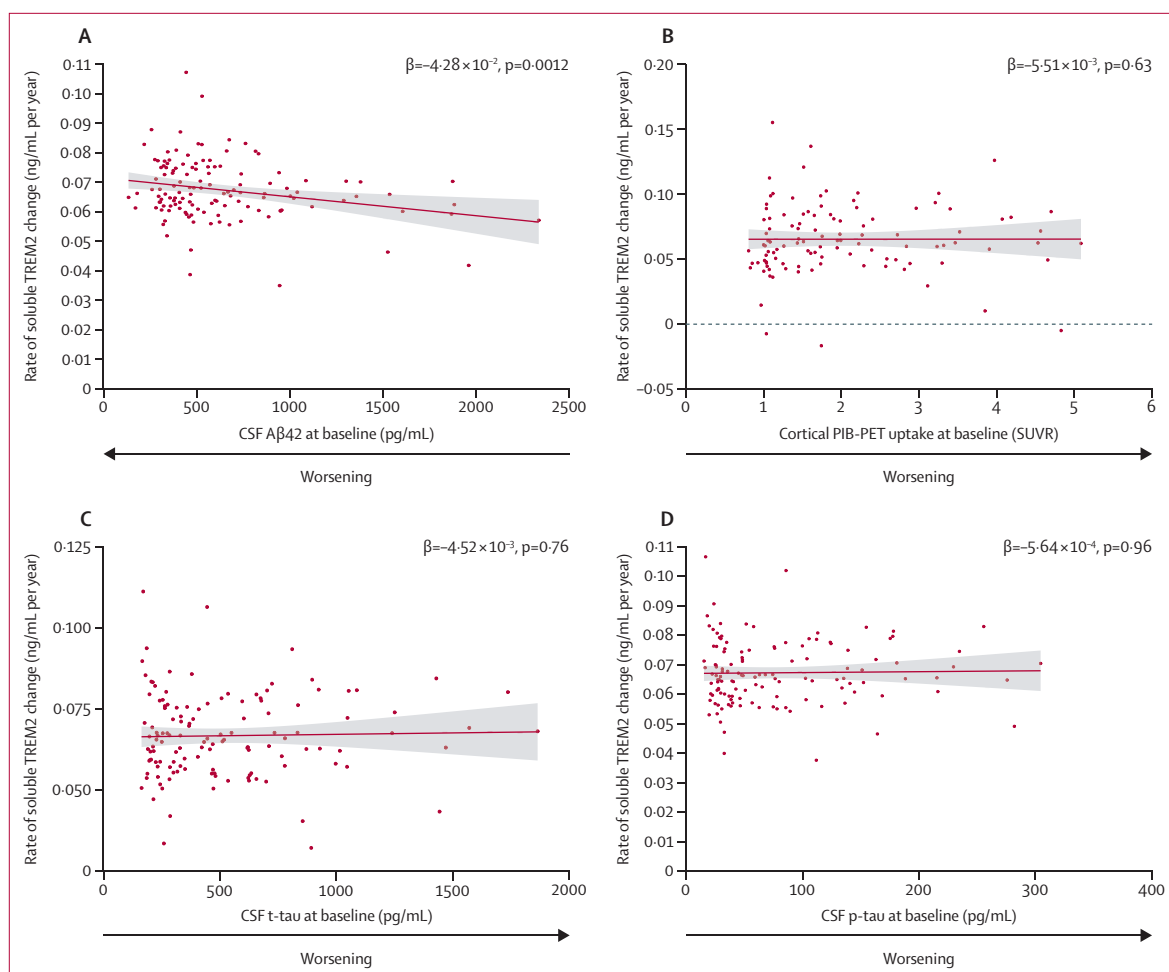


**Figure 2: Baseline A $\beta$ 42, p-tau, t-tau in CSF, and PiB-PET and rate of change in soluble TREM2 in CSF in carriers of pathogenic variants**

Each panel represents the estimated individual slopes extracted from the respective separate univariate linear mixed effects (LME) models, which assessed the association between the baseline predictor biomarker (A $\beta$ 42 in CSF [A], PiB-PET cortical uptake [B], t-tau in CSF [C], and p-tau in CSF [D]), and the subsequent longitudinal change in soluble TREM2 in CSF.  $\beta$  values and p values indicate the effect and statistical significance of the interaction term time from baseline  $\times$  predictor-baseline-biomarker in each separate univariate LME model. The interaction term represents the effect of the baseline biomarker on the longitudinal change in soluble TREM2 in CSF. The separate univariate LME model is explained further in the appendix (p 13). Each univariate LME model consisted of longitudinal CSF soluble TREM2 as the dependent variable (ie, the outcome), time from-baseline, estimated years to symptom onset (EYO) at baseline, predictor biomarker at baseline and interactions Time  $\times$  EYO at baseline and Time  $\times$  Predictor at baseline as fixed factors and individual slope, intercept, and family cluster as random factors. Continuous red lines represent the association between the individual slopes, which were estimated from the univariate LME models and the baseline biomarker. Bands represent 95% CI. (A) Low baseline amounts of A $\beta$ 42 in CSF were associated with a subsequent augmented rate of change in soluble TREM2, according to the respective LME model. For total cortical PiB-PET uptake at baseline (B), baseline t-tau in CSF (C), and baseline p-tau in CSF (D), we did not find any significant effect on the subsequent rate of soluble TREM2 change estimated by the LME models (appendix p 13). PiB-PET=Pittsburgh compound B PET. p-tau=phosphorylated tau on threonine 181. SUVR=standardised uptake value ratio. t-tau=total tau.

functional, clinical, and therapeutically insightful observations.

First, we found that low levels at baseline of A $\beta$ 42 in CSF, and a low ratio of A $\beta$ 42 to A $\beta$ 40 in CSF, were associated with an augmented rate of increase in soluble TREM2, but not with high baseline cortical PiB-PET uptake nor with markers for tau-related pathology or neuronal death. This finding suggests that very early A $\beta$  seeding, even before amyloid-PET imaging detects any A $\beta$  plaque deposition, triggers soluble TREM2 generation. In fact, very early A $\beta$  aggregation before seeds are detectable by histology has been described in

animal models.<sup>31</sup> This novel finding also accords with previous findings in mouse models, which showed that the smallest A $\beta$  deposits are sensed and removed by microglia in a TREM2-dependent manner.<sup>22</sup> Our previous cross-sectional study suggested a much later increase of soluble TREM2 than did the results of this study, only 5 years before the expected onset.<sup>8</sup> However, compared with our previous work, the greater statistical power of our current analytical method<sup>19,23</sup> (which is based on an LME model incorporating both cross-sectional and longitudinal data), the larger sample size, and the higher sensitivity and specificity of our novel immunoassay

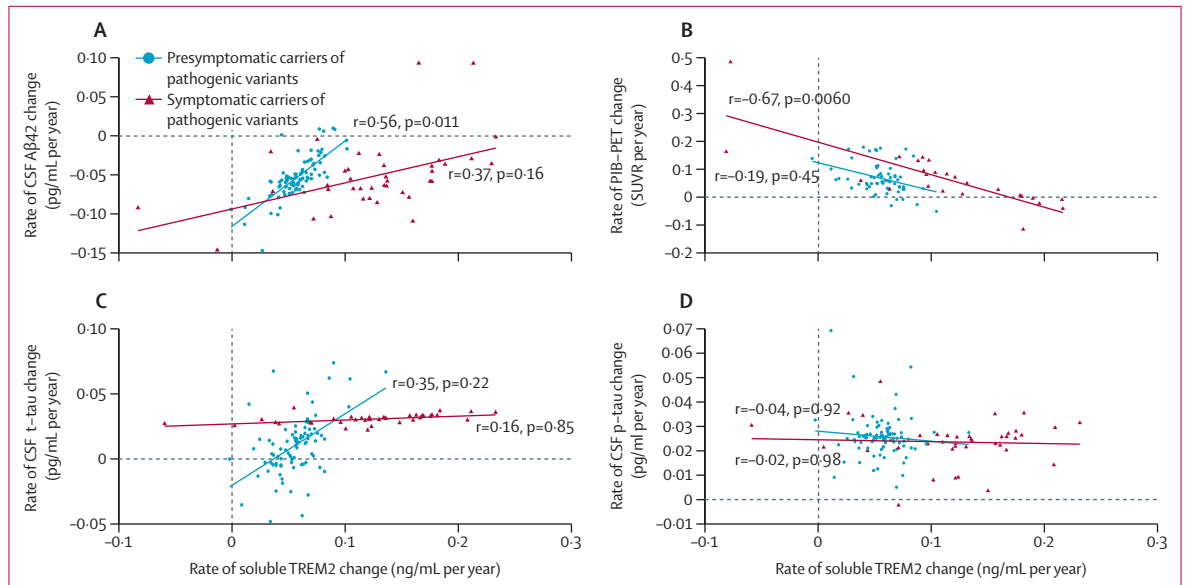


**Figure 3: Association in carriers of pathogenic variants between rate of increase in soluble TREM2 and rates of change of biomarkers related to amyloid deposition and tau-related pathology**

(A) Augmented rates of increase in soluble TREM2 correlated with a diminished rate of decrease in Aβ42 in CSF, in presymptomatic carriers of pathogenic variants (shown in blue, n=100). No significant correlation was found in symptomatic carriers of pathogenic variants (shown in dark red, n=48). (B) A significant association between an augmented rate of increase in soluble TREM2 and a reduced rate of increase in cortical PiB-PET uptake was observed in symptomatic carriers of pathogenic variants (shown in dark red, n=48). When studying all carriers of pathogenic variants together, we also observed a significant association ( $r=-0.46, p=0.0068$ ). (C) No evidence for an association between augmented rates of increase in soluble TREM2 and t-tau was observed on studying all carriers of pathogenic variants together ( $r=0.34, p=0.0800$ ). (D) No significant association between the rate of change in soluble TREM2 and the rate of change in p-tau in carriers of pathogenic variants was observed (neither in presymptomatic or symptomatic carriers of pathogenic variants, nor in the entire pathogenic variant group). Presymptomatic carriers of pathogenic variants were defined by a CDR at baseline of 0, and symptomatic carriers of pathogenic variants were defined by a CDR at baseline greater than 0. Datapoints on the plots represent individual annual rates of change for each variable, which were estimated from their corresponding bivariate LME model. The correlations ( $r$ ) between each pair of rates of change, and corresponding  $p$  values, were estimated from the covariance matrix of each separate bivariate LME model. The continuous lines in each panel represent the linear association between the annual rate of change of soluble TREM2 and another outcome. CDR=Clinical Dementia Rating. LME=linear mixed effects. PiB-PET=Pittsburgh compound B PET. p-tau=phosphorylated tau on threonine 181. SUVR=standardised uptake value ratio. t-tau=total tau.

allowed us to detect augmented soluble TREM2 levels in symptomatic carriers of pathogenic variants compared with non-carriers up to 21 years before expected symptom onset. This timepoint of 21 years before the expected symptom onset is very close to the timepoint at which longitudinal changes in amyloid markers start to diverge in symptomatic carriers of pathogenic variants compared with non-carriers (25 years before symptom onset for amyloid-PET and 24 years before symptom onset CSF Aβ42).<sup>19,23</sup> These findings support the notion that the microglial response is very sensitive to the slightest amyloid-related pathological challenges.

We also showed that an augmented annual rate of increase in soluble TREM2 was associated with a diminished annual rate of decrease in Aβ42 in CSF in presymptomatic carriers of pathogenic variants, and a reduced annual rate of increase in PiB-PET cortical uptake in symptomatic carriers of pathogenic variants. These selective associations, depending on the clinical phase, support a potential dual protective effect aimed at reducing plaque-associated toxicity, which accords with previous findings in animal models.<sup>22,32</sup> In the early presymptomatic stages of Alzheimer's disease, the association between an augmented annual rate of increase in soluble TREM2 and

a diminished annual rate of decrease in Aβ42 in CSF might be related to microglia clustering around the smallest Aβ seeds, reducing their ability to grow and spread.<sup>22</sup> When plaques are fully developed, a protective function of microglia might be carried out by their barrier function and their ability to compact Aβ plaques, possibly driven by co-aggregation of Aβ and microglial-released APOE.<sup>22,32,33</sup> This hypothesis is also supported by our previous findings, in which high levels of soluble TREM2 at baseline predicted a diminished annual rate of amyloid-PET uptake.<sup>12</sup> In line with these findings, we found that having augmented or diminished annual rates of increase in soluble TREM2 affected the association between longitudinal changes in Aβ42 in CSF and PiB-PET uptake in presymptomatic carriers of pathogenic variants. Thus, individuals with reduced annual rates of increase in soluble TREM2 had augmented rates of uptake of PiB-PET signal related to longitudinal rises in amounts of Aβ42 in CSF, while individuals with augmented annual rates of increase in soluble TREM2 had the opposite relationship. Furthermore, although no association between longitudinal changes in Aβ42 in CSF and amyloid-PET imaging has been found so far,<sup>34</sup> we obtained an accurate model to predict changes in these markers



when we introduced the interaction between PiB-PET and soluble TREM2 in the model. These findings highlight the important role of TREM2 in A $\beta$  plaque metabolism and point to the relevance of soluble TREM2 for the interpretation of amyloid markers in the clinical setting.

Regarding tau-related Alzheimer's disease pathology, we did not detect any significant association between baseline levels of tau-related markers and the subsequent longitudinal increase in soluble TREM2. Previous cross-sectional studies in both sporadic and genetic Alzheimer's disease cohorts showed a strong correlation between soluble TREM2 and t-tau and p-tau,<sup>8–10,27</sup> highlighting the differences between longitudinal and cross-sectional approaches to assess different aspects of the association between biomarkers. We interpret this cross-sectional correlation as the static view of Alzheimer's disease development, in which both markers are sequentially higher as a result of A $\beta$  deposition, reflecting disease progression. Importantly, we found that an augmented longitudinal increase in soluble TREM2 attenuated the longitudinal rise in p-tau related to the rate of uptake of PiB-PET in presymptomatic carriers of pathogenic variants, suggesting a potential protective role of TREM2 function on amyloid-dependent tau pathology, in line with results in mouse models.<sup>35</sup>

According to the protective effects of TREM2 on both amyloid-related and tau-related pathology, the augmented longitudinal increase in soluble TREM2 correlated with slower cortical shrinkage in the precuneus, in presymptomatic carriers of pathogenic variants. Although high baseline soluble TREM2 levels predicted a diminished rate of hippocampal shrinkage in carriers of pathogenic variants, in accordance with previous studies,<sup>13</sup> we could not detect an association between a longitudinal change in soluble TREM2 and longitudinal shrinkage of hippocampal volume. Of note, the precuneus is the first region affected by A $\beta$  accumulation in autosomal dominant Alzheimer's disease, followed by a decrease in cortical fluorodeoxyglucose-(FDG)PET signal and subsequent cortical shrinkage.<sup>23</sup> This canonical sequence is not followed in the hippocampal region, where atrophy is the main event.<sup>23</sup> The beneficial TREM2 effect could have a regional pattern, being more evident at an early stage in brain areas with an augmented rate of A $\beta$  accumulation, which supports the triggering of TREM2 protective functions by early A $\beta$  aggregation.

Finally, we found a very striking correlation between an augmented longitudinal increase in soluble TREM2 and a decelerated rate of cognitive decline in people with presymptomatic Alzheimer's disease. This result accorded with the association noted between an augmented longitudinal increase in soluble TREM2 and a reduced rate of pathological progression in the presymptomatic phase of the disease, represented by a diminished rate of decrease in A $\beta$ 42 in CSF and a decelerated rate of cortical shrinkage in the precuneus. These findings highlight the association between amyloid pathology, neurodegeneration, and

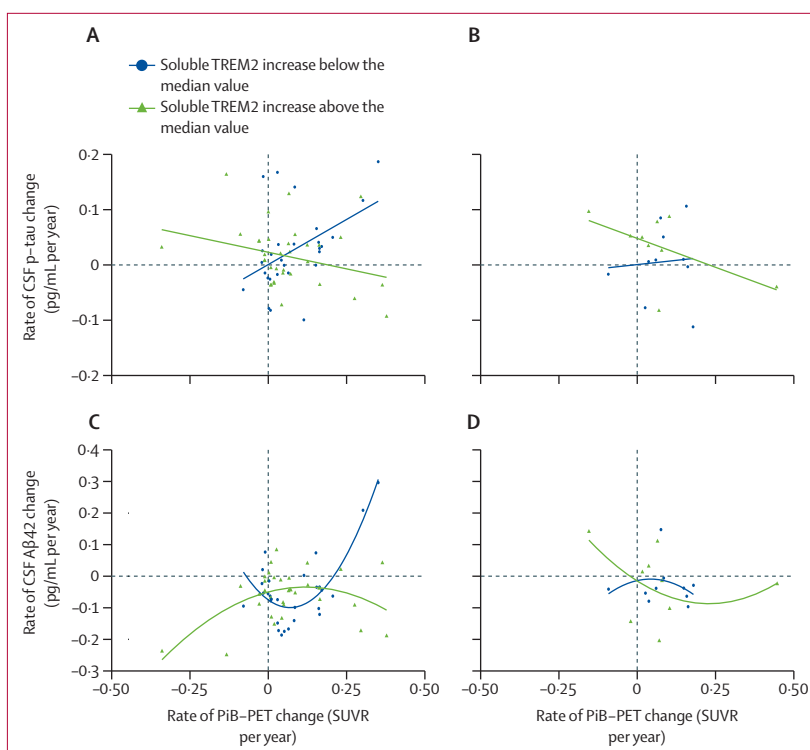


**Figure 4: Modification effect of rate of increase in soluble TREM2 on associations between longitudinal changes in PiB-PET cortical uptake, A $\beta$ 42 in CSF, and p-tau in CSF**

(A) In presymptomatic carriers of pathogenic variants, the association between raw rates of change in PiB-PET uptake and p-tau in CSF was modified by the raw rate of change in soluble TREM2 ( $\beta = -0.394$  [0.137],  $p = 0.0056$ , for the linear interaction of rate of increase in soluble TREM2 higher than the median  $\times$  annual rate of increase in PiB-PET), with opposite associations in the subgroup with a low rate of increase in soluble TREM2 (below the median [shown in blue],  $n = 50$ ) and the subgroup with a high rate (above the median [shown in green],  $n = 48$ ). (B) This interaction effect was not significant in symptomatic carriers of pathogenic variants ( $\beta = -0.271$  [0.288],  $p = 0.36$ ). (C) Presymptomatic carriers of pathogenic variants with a high rate of change in soluble TREM2 (above the median [shown in green],  $n = 50$ ) and those with a low rate of change in soluble TREM2 (shown in blue,  $n = 48$ ) showed opposite associations between longitudinal changes in A $\beta$ 42 in CSF and PiB-PET uptake ( $\beta = 0.974$  [SE 0.318],  $p = 0.0033$  for the linear interaction term of increase in soluble TREM2 higher than the median  $\times$  annual rate of increase in PiB-PET, and  $\beta = -6.24$  [1.135],  $p < 0.0001$  for the quadratic interaction term of increase in soluble TREM2 higher than the median  $\times$  annual rate of increase in PiB-PET<sup>2</sup>). (D) This interaction effect was not significant in symptomatic carriers of pathogenic variants ( $\beta = -2.11$  [3.95],  $p = 0.61$  for the linear interaction term rate of increase in soluble TREM2 higher than the median  $\times$  annual rate of increase in PiB-PET, and  $\beta = -0.63$  [0.54],  $p = 0.27$  for the quadratic interaction term of increase in soluble TREM2 higher than the median  $\times$  annual rate of increase in PiB-PET<sup>2</sup>). Datapoints on the plots represent the raw rates of change of each biomarker, which were calculated as the individual slope per participant in a linear regression (ie, biomarker of study by time).  $\beta$  values in each panel are the  $\beta$  coefficient for the linear and quadratic interaction terms in each linear or quadratic regression model. The exact regression models carried out are summarised in the appendix (p 14). The SE is expressed in parentheses. The continuous lines in each panel are linear or quadratic estimates of the represented data. PiB-PET = Pittsburgh compound B PET. p-tau = phosphorylated tau on threonine 181.

consequent cognitive decline. We noted that high baseline soluble TREM2 levels exerted a beneficial effect on memory domains in people with symptomatic sporadic Alzheimer's disease, which was in line with the reported association between high amounts at baseline of soluble TREM2 and decreased hippocampal shrinkage.<sup>13</sup> We could not detect such effects of baseline soluble TREM2 levels on cognition in our current study, possibly because of the different cognitive composite measure used, which is not specific for memory domains, and because our current study was focused on the presymptomatic Alzheimer's disease phase. Taken together, our results suggest that an

augmented rate of increase in soluble TREM2 in the presymptomatic Alzheimer's disease stage slows A $\beta$  deposition and precuneus shrinkage, leading to a clear clinical readout via its strong association with a slower cognitive decline. The beneficial effect of TREM2 functions

might continue in symptomatic stages by slowing hippocampal shrinkage in individuals with the highest levels in CSF of soluble TREM2.

The main limitation of our study is that we used an observational cohort. Thus, any causative associations

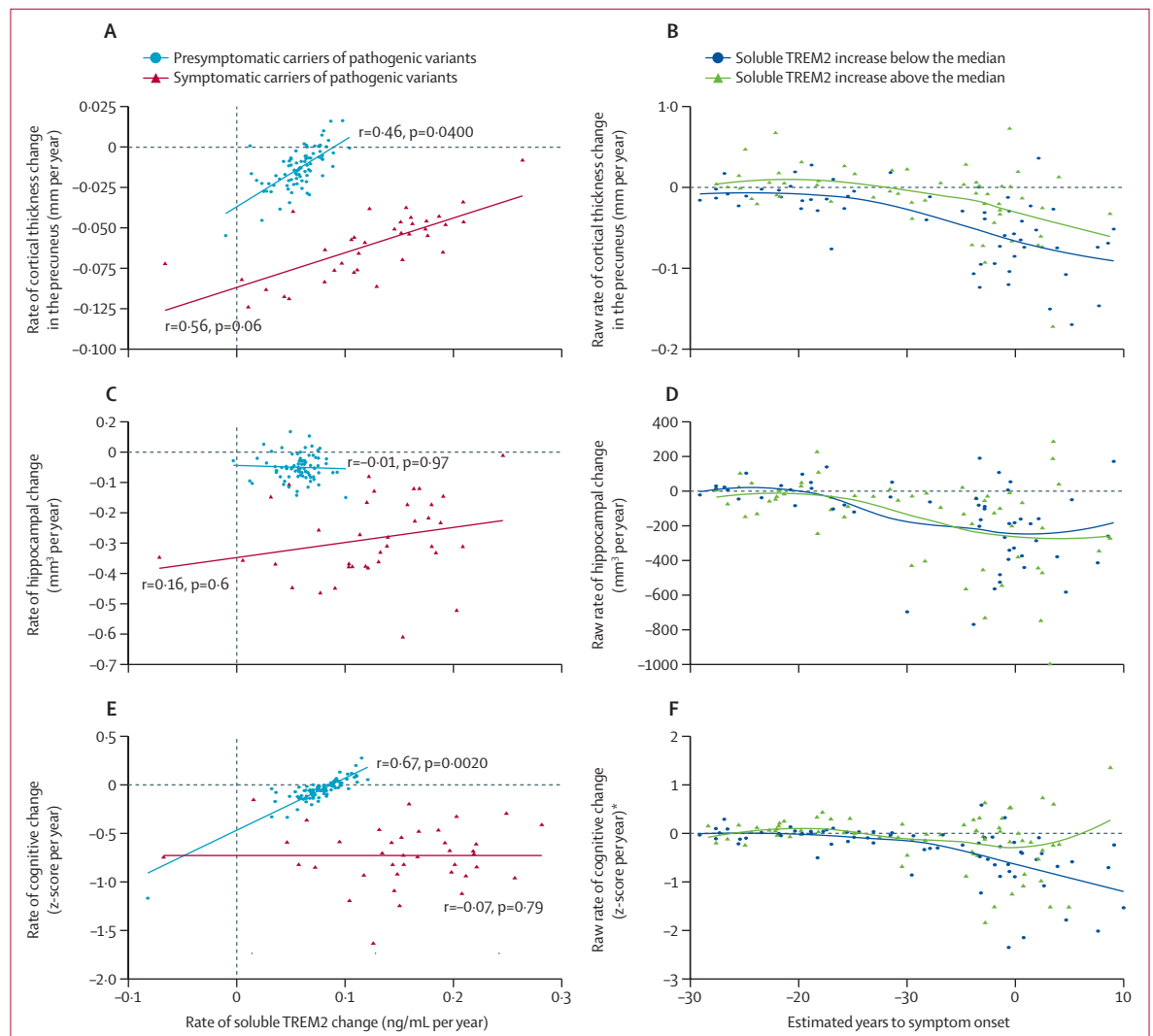


**Figure 5: Associations between rate of increase in soluble TREM2, cortical shrinkage in the precuneus, hippocampal shrinkage, and cognitive decline in presymptomatic and symptomatic carriers of pathogenic variants**

(A) A significant association was seen between an augmented rate of increase in soluble TREM2 and decreased cortical shrinkage in the precuneus, in presymptomatic carriers of pathogenic variants (shown in blue,  $n=100$ ), and weak evidence was noted for a similar potential association in symptomatic carriers of pathogenic variants (shown in dark red,  $n=48$ ). (B) The raw rate of cortical shrinkage in the precuneus is shown (for illustrative purposes only) according to EYO in carriers of pathogenic variants. Carriers of pathogenic variants were divided into two groups according to their raw rate of change in soluble TREM2 (above the median [shown in green], and below the median [shown in blue]). (C) There was no significant association between the rate of increase in soluble TREM2 and the hippocampal shrinkage rate in presymptomatic or symptomatic carriers of pathogenic variants. (D) The raw rate of hippocampal shrinkage according to EYO in carriers of pathogenic variants is shown (for illustrative purposes only), divided into two groups according to raw rate of change in soluble TREM2 (above the median [shown in green], and below the median [shown in blue]). (E) A strong correlation between higher soluble TREM2 increase rates and slower cognitive decline was observed in presymptomatic carriers of pathogenic variants (shown in blue,  $n=100$ ), but not in the symptomatic carriers of pathogenic variants (shown in dark red,  $n=48$ ). (F) The raw rate of cognitive decline according to EYO in carriers of pathogenic variants is shown (for illustrative purposes only), divided into two groups according to their raw rate of soluble TREM2 (above the median [shown in green], and below the median [shown in blue]). The raw rates of change were calculated as the individual slope per participant in a linear regression (ie, biomarker or cognitive composite by time). The correlations ( $r$ ) between each pair of rates of change in panels A, C, and E, and the correspondent  $p$  values, were estimated from the covariance matrix of each separate bivariate LME model. The rates of change represented in panels B, D, and E were extracted from the correspondent bivariate LME model. The continuous lines in each panel are linear estimates of the represented data. The dashed lines in panels B, D, and F indicate that the change was equal to zero, indicating stability. CDR=Clinical Dementia Rating. EYO=estimated years to symptom onset. LME=linear mixed effects. \*The cognitive change was calculated on the basis of the cognitive composite already described.<sup>28</sup>

must be interpreted with caution. Additionally, replication of our findings in the presymptomatic phase of sporadic late-onset Alzheimer's disease is impossible because of the lack of a suitable large cohort with sufficient follow-up of at least two decades from first pathological changes to disease onset. Moreover, we used various biomarkers, which are indirect measures for studying pathological processes. Furthermore, the study of the association between longitudinal changes of tau-related markers and soluble TREM2 was restricted to CSF markers, with no available tau imaging. Additionally, soluble TREM2 is only an indirect biomarker of TREM2 signaling, which does not allow any conclusions to be made on regional changes in microglial activity. No biomarker readouts for downstream TREM2 signaling are currently available to monitor cell autonomous TREM2-dependent microglial activation. We also must consider that numerous genetic contributors could have affected soluble TREM2 levels. For example, ADAM10-generated soluble TREM2 could be modulated by factors affecting  $\alpha$ -secretase activity (eg, epigenetic factors or different factors acting at the transcriptional, translational, or post-translational level).<sup>36</sup> Furthermore, the *MS4A* gene cluster is associated with soluble TREM2 concentrations in CSF. Strikingly, within this cluster, variants associated with high levels of soluble TREM2 in CSF are associated with a later symptom onset in Alzheimer's disease.<sup>11</sup> Other trafficking factors that either guide TREM2 to the surface or assist with TREM2 clearance could also affect generation of soluble TREM2.<sup>37</sup> However, such genetic factors, linked to individual patients, can affect total amounts in CSF of soluble TREM2, but have less effect on the individual longitudinal rate of increase.

One of the main strengths of our study is its longitudinal design. With this design, we could report a comprehensive and complete set of highly consistent findings, including biological triggers of the increase in soluble TREM2 and its effects on amyloid deposition, tau-related pathology, brain structure, and cognition, which are not possible to investigate with a cross-sectional approach. Our findings also have implications for the future design of clinical trials and the interpretation of amyloid-related pathological markers. The very early response of microglia to A $\beta$  aggregation emphasises the importance of beginning any treatment for Alzheimer's disease within the presymptomatic phase, immediately after biomarker-based evidence of amyloid pathology is recorded. Moreover, soluble TREM2 in CSF could have an important stratification value within clinical trials. For example, patients with low rates of increase in soluble TREM2 might have a better outcome on therapeutic TREM2 modulation than might those with high rate of increase of soluble TREM2 in CSF at an early disease stage, which subsequently might not increase any further. Furthermore, the direct association between soluble TREM2 and amyloid deposition not only supports the notion of combination

treatment with anti-amyloid and microglia-modulating therapies but also points to soluble TREM2 in CSF as a potential key marker within anti-amyloid clinical trials. Finally, according to our results, the induction of microglial TREM2 activity should be placed right after the earliest deposition of amyloid plaques, possibly immediately after or even during the seeding process. Thus, our results support TREM2-dependent microglial activation as an integral part of the amyloid cascade.

#### Contributors

MS-C, EM-R, and CH designed the study. EM-R and BNU carried out the soluble TREM2 measurements. EM-R, YL, and NF had full access to raw data. EM-R and YL carried out the final statistical analyses. YL, CX, and RJB accessed and verified the underlying data. EM-R and CH wrote the manuscript and had the final responsibility to submit for publication. RF generated the neoepitope specific monoclonal antibodies. EM-R, GK, and KS developed the new Meso Scale Discovery-immunoassay. KB, BNE, and HZ provided CSF samples to validate the new Meso Scale Discovery-immunoassay. All other coauthors contributed CSF samples and clinical data from the Dominantly Inherited Alzheimer's Network (DIAN) participants. All coauthors contributed to the interpretation of the results and critically reviewed the manuscript.

#### Declaration of interests

HZ has served at scientific advisory boards for Alector, Eisai, Denali, Roche Diagnostics, Wave, Samumed, Siemens Healthineers, Pinteon Therapeutics, Nervgen, AZTherapies, and CogRx, and has given lectures in symposia sponsored by Cellectricon, Fujirebio, Alzecure, and Biogen. MS-C has served as a consultant and at advisory boards for Roche Diagnostics International and has given lectures in symposia sponsored by Roche Diagnostics, Sociedad Limitada Unipersonal, and Roche Farma, Sociedad Anónima. AMF participates in the scientific advisory boards for Roche Diagnostics, Genentech, and DiamiR, and collaborates as a consultant for DiamiR and Siemens Healthcare Diagnostics. TLSB collaborates with Biogen and Siemens as a consultant and participates in the Advisory board of Eisai and Biogen. JH collaborates as a consultant for Roche and Paragon Nanolabs, and participates in the Advisory board of Eisai, CaringBridge, and WallE. EM collaborates as a consultant for Eli Lilly, has received funding for attending meetings from the Alzheimer Association and Foundation Alzheimer, and participates in the Data Safety Monitoring Board of Eli Lilly, Alector, and in the Advisory Board of Fondation Alzheimer, and Alzmemd. KS received royalties for co-developing the therapeutic anti-TREM2 mouse antibody 4D9. JCM has served as consultant for Barcelona Beta Brain Research Center, TS Srinivasan Advisory Board (Chennai, India), has received honoraria for lectures given at Montefiori Grand Rounds (NY, USA) and Tetra-Institute Alzheimer Disease Research Center Seminar Series, and participates in the Advisory Boards of Cure Alzheimer's Fund Research Strategy Council and Leads Advisory Board (IN, USA). KB collaborates as a consultant for Abcam, Axon, BioArctic, Biogen, Japanese Organization for Medical Device Development and Shimadzu, Lilly, MagQu, Pharmatrophix, Prothena, Roche Diagnostics, and Siemens Healthineers, has received honoraria for lectures from Grupo de Estudos de Envelhecimento Cerebral e Demência and Roche Diagnostics, and IFCC and SNIBE, has served at data monitoring committees for Julius Clinical and Novartis, and is a co-founder of Brain Biomarker Solutions in Gothenburg AB, which is a part of Gothenburg University Ventures Incubator programme. JL participates as a consultant in Axon Neuroscience and Biogen, has received honoraria for lectures given by Bayer Vital and Roche, support for attending meetings by AbbVie and Biogen, and has participated in the Advisory board of Axon Neuroscience. JL has also received author fees from Thieme medical publishers, W Kohlhammer GmbH medical publishers, and a compensation for duty as part-time chief marketing officer by MODAG GmbH. RJB collaborates as a consultant with Eisai, Amgen, and Hoffman La-Roche, has received travel support from Hoffman La-Roche, and participates in the C2N Diagnostics Scientific Advisory board. RJB also serves as principal investigator of the Dominantly Inherited Alzheimer's Network-Treatment Unit (DIAN-TU), which is supported by the Alzheimer's Association, GHR Foundation, an anonymous organisation,

and the DIAN-TU Pharma Consortium (active members include Eli Lilly and Company, Avid Radiopharmaceuticals, F Hoffman-La Roche, Genentech, Biogen, Eisai, and Janssen. Previous members include Abbvie, Amgen, AstraZeneca, Forum, Mithridion, Novartis, Pfizer, Sanofi, and United Neuroscience). In addition, in-kind support has been received from CogState and Signant Health. CH collaborates with Denali Therapeutics, and has participated on one advisory board meeting of Biogen. CH is also chief advisor of ISAR Bioscience and a member of the scientific advisory board of AviadoBio. CH has received honoraria for lectures at Weill Cornell Medicine, Sheikh Hamdan Webinar Series, Washington University, Eisai, and UT Southwestern Medical Center, and participates in the US Patent Application (number 16/319,373).

#### Data sharing

All the data used in this study are available on request from DIAN at: <https://dian.wustl.edu/our-research/observational-study/dianobservational-study-investigator-resources/>. The codes used for data analysing in our study can be requested from the corresponding author (CH).

#### Acknowledgments

Data collection and sharing for this project was supported by The Dominantly Inherited Alzheimer's Network (DIAN, UF1AG032438) funded by the National Institute on Aging, the German Center for Neurodegenerative Diseases, Raul Carrera Institute for Neurological Research, Partial support by the Research and Development Grants for Dementia from Japan Agency for Medical Research and Development, and the Korea Health Technology R&D Project through the Korea Health Industry Development Institute. This manuscript has been reviewed by DIAN study investigators for scientific content and consistency of data interpretation with previous DIAN study publications. We acknowledge the altruism of the participants and their families and contributions of the DIAN research and support staff at each of the participating sites for their contributions to this study. We thank Lis de Weerd and Sophie Robinson for critically reading the manuscript. TREM2 related work is supported by a Koselleck Project grant (HA1737/16-1) awarded to CH and DIAN (UF1AG032438; principal investigator, RB). CH and RF are supported by the Deutsche Forschungsgemeinschaft (German Research Foundation) under Germany's Excellence Strategy within the framework of the Munich Cluster for Systems Neurology (EXC 2145 SyNergy; ID 390857198). HZ is a Wallenberg Scholar supported by grants from the Swedish Research Council (2018-02532), the European Research Council (681712), and Swedish State Support for Clinical Research (ALFGBG-720931). MS-C is funded by the European Research Council under the European Union's Horizon 2020 research and innovation programme (grant agreement number 948677). MS-C also receives funding from the Instituto de Salud Carlos III (PI19/00155) and from the Spanish Ministry of Science, Innovation and Universities (Juan de la Cierva Programme grant IJC2018-037478-I). KB is supported by the Swedish Research Council (2017-00915), the Alzheimer Drug Discovery Foundation (RDAPB-201809-2016615), the Swedish Alzheimer Foundation (AF-742881), Hjärnfonderna (FO2017-0243), the Swedish state under the agreement between the Swedish government and the County Councils, the ALF-agreement (ALFGBG-715986), the European Union Joint Program for Neurodegenerative Disorders (JPN2019-466-236), the National Institute of Health (grant number 1R01AG068398-01), and the Alzheimer's Association 2021 Zenith Award (ZEN-21-848495).

#### References

- Heneka MT, Kummer MP, Stutz A, et al. NLRP3 is activated in Alzheimer's disease and contributes to pathology in APP/PS1 mice. *Nature* 2013; **493**: 674–78.
- Keren-Shaul H, Spinrad A, Weiner A, et al. A unique microglia type associated with restricting development of Alzheimer's disease. *Cell* 2017; **169**: 1276–1290.e17.
- Guerreiro R, Wojtas A, Bras J, et al. TREM2 variants in Alzheimer's disease. *N Engl J Med* 2013; **368**: 117–27.
- Kleinberger G, Yamanishi Y, Suárez-Calvet M, et al. TREM2 mutations implicated in neurodegeneration impair cell surface transport and phagocytosis. *Sci Transl Med* 2014; **6**: 243ra86.
- Mazaheri F, Snaidero N, Kleinberger G, et al. TREM2 deficiency impairs chemotaxis and microglial responses to neuronal injury. *EMBO Rep* 2017; **18**: 1186–98.
- Lewcock JW, Schlepckow K, Di Paolo G, Tahirovic S, Monroe KM, Haass C. Emerging microglia biology defines novel therapeutic approaches for Alzheimer's disease. *Neuron* 2020; **108**: 801–21.
- Schlepckow K, Kleinberger G, Fukumori A, et al. An Alzheimer-associated TREM2 variant occurs at the ADAM cleavage site and affects shedding and phagocytic function. *EMBO Mol Med* 2017; **9**: 1356–65.
- Suárez-Calvet M, Araque Caballero MA, Kleinberger G, et al. Early changes in CSF sTREM2 in dominantly inherited Alzheimer's disease occur after amyloid deposition and neuronal injury. *Sci Transl Med* 2016; **8**: 369ra178.
- Suárez-Calvet M, Kleinberger G, Araque Caballero MA, et al. sTREM2 cerebrospinal fluid levels are a potential biomarker for microglia activity in early-stage Alzheimer's disease and associate with neuronal injury markers. *EMBO Mol Med* 2016; **8**: 466–76.
- Piccio L, Deming Y, Del-Águila JL, et al. Cerebrospinal fluid soluble TREM2 is higher in Alzheimer disease and associated with mutation status. *Acta Neuropathol* 2016; **131**: 925–33.
- Deming Y, Filipello F, Cignarella F, et al. The MS4A gene cluster is a key modulator of soluble TREM2 and Alzheimer's disease risk. *Sci Transl Med* 2019; **11**: eaau2291.
- Ewers M, Biechele G, Suárez-Calvet M, et al. Higher CSF sTREM2 and microglia activation are associated with slower rates of beta-amyloid accumulation. *EMBO Mol Med* 2020; **12**: e12308.
- Ewers M, Franzmeier N, Suárez-Calvet M, et al. Increased soluble TREM2 in cerebrospinal fluid is associated with reduced cognitive and clinical decline in Alzheimer's disease. *Sci Transl Med* 2019; **11**: eaav6221.
- Pascoal TA, Benedet AL, Ashton NJ, et al. Microglial activation and tau propagate jointly across Braak stages. *Nat Med* 2021; **27**: 1592–99.
- Zhang PF, Hu H, Tan L, Yu JT. Microglia biomarkers in Alzheimer's disease. *Mol Neurobiol* 2021; **58**: 3388–404.
- Edwin TH, Henjum K, Nilsson LNG, et al. A high cerebrospinal fluid soluble TREM2 level is associated with slow clinical progression of Alzheimer's disease. *Alzheimers Dement (Amst)* 2020; **12**: e12128.
- Falcon C, Monté-Rubio GC, Grau-Rivera O, et al. CSF glial biomarkers YKL40 and sTREM2 are associated with longitudinal volume and diffusivity changes in cognitively unimpaired individuals. *Neuroimage Clin* 2019; **23**: 101801.
- Xu Z, Shen X, Pan W. Longitudinal analysis is more powerful than cross-sectional analysis in detecting genetic association with neuroimaging phenotypes. *PLoS One* 2014; **9**: e102312.
- McDade E, Wang G, Gordon BA, et al. Longitudinal cognitive and biomarker changes in dominantly inherited Alzheimer disease. *Neurology* 2018; **91**: e1295–306.
- Schmitz TW, Soreq H, Poirier J, Spreng RN. Longitudinal basal forebrain degeneration interacts with TREM2/C3 biomarkers of inflammation in presymptomatic Alzheimer's disease. *J Neurosci* 2020; **40**: 1931–42.
- Bartl M, Dakna M, Galasko D, et al. Biomarkers of neurodegeneration and glial activation validated in Alzheimer's disease assessed in longitudinal cerebrospinal fluid samples of Parkinson's disease. *PLoS One* 2021; **16**: e0257372.
- Parhizkar S, Arzberger T, Brendel M, et al. Loss of TREM2 function increases amyloid seeding but reduces plaque-associated ApoE. *Nat Neurosci* 2019; **22**: 191–204.
- Gordon BA, Blazey TM, Su Y, et al. Spatial patterns of neuroimaging biomarker change in individuals from families with autosomal dominant Alzheimer's disease: a longitudinal study. *Lancet Neurol* 2018; **17**: 241–50.
- Bateman RJ, Xiong C, Benzinger TL, et al. Clinical and biomarker changes in dominantly inherited Alzheimer's disease. *N Engl J Med* 2012; **367**: 795–804.
- Tsubuki S, Takaki Y, Saido TC. Dutch, Flemish, Italian, and Arctic mutations of APP and resistance of Abeta to physiologically relevant proteolytic degradation. *Lancet* 2003; **361**: 1957–58.
- Morris JC. The Clinical Dementia Rating (CDR): current version and scoring rules. *Neurology* 1993; **43**: 2412–14.
- Suárez-Calvet M, Morenas-Rodríguez E, Kleinberger G, et al. Early increase of CSF sTREM2 in Alzheimer's disease is associated with tau related-neurodegeneration but not with amyloid-β pathology. *Mol Neurodegener* 2019; **14**: 1.
- Bateman RJ, Benzinger TL, Berry S, et al. The DIAN-TU Next Generation Alzheimer's prevention trial: adaptive design and disease progression model. *Alzheimers Dement* 2017; **13**: 8–19.

- 29 Fieuws S, Verbeke G. Joint modelling of multivariate longitudinal profiles: pitfalls of the random-effects approach. *Stat Med* 2004; **23**: 3093–104.
- 30 Luo J, Gao F, Liu J, et al. Statistical estimation and comparison of group-specific bivariate correlation coefficients in family-type clustered studies. *J Appl Stat* 2021; published online March. doi:10.1080/02664763.2021.1899141.
- 31 Uhlmann RE, Rother C, Rasmussen J, et al. Acute targeting of pre-amyloid seeds in transgenic mice reduces Alzheimer-like pathology later in life. *Nat Neurosci* 2020; **23**: 1580–88.
- 32 Huang Y, Happonen KE, Burrola PG, et al. Microglia use TAM receptors to detect and engulf amyloid  $\beta$  plaques. *Nat Immunol* 2021; **22**: 586–94.
- 33 Meilandt WJ, Ngu H, Gogineni A, et al. Trem2 deletion reduces late-stage amyloid plaque accumulation, elevates the A $\beta$ 42:A $\beta$ 40 ratio, and exacerbates axonal dystrophy and dendritic spine loss in the PS2APP Alzheimer's mouse model. *J Neurosci* 2020; **40**: 1956–74.
- 34 Toledo JB, Bjerke M, Da X, et al. Nonlinear association between cerebrospinal fluid and florbetapir F-18  $\beta$ -amyloid measures across the spectrum of Alzheimer disease. *JAMA Neurol* 2015; **72**: 571–81.
- 35 Lee SH, Meilandt WJ, Xie L, et al. Trem2 restrains the enhancement of tau accumulation and neurodegeneration by  $\beta$ -amyloid pathology. *Neuron* 2021; **109**: 1283–301.e6.
- 36 Kunkle BW, Grenier-Boley B, Sims R, et al. Genetic meta-analysis of diagnosed Alzheimer's disease identifies new risk loci and implicates A $\beta$ , tau, immunity and lipid processing. *Nat Genet* 2019; **51**: 414–30.
- 37 Small SA, Petsko GA. Endosomal recycling reconciles the Alzheimer's disease paradox. *Sci Transl Med* 2020; **12**: eabb1717.